This is a manuscript of an article that was accepted in April 2017 for publication in the Journal of Hydrologic Engineering

Effect of rain gauge proximity on rainfall estimation for problematic urban coastal watersheds in Virginia Beach, VA USA

Jeffrey M. Sadler[1], Jonathan L. Goodall, Ph.D., PE.[2], and Mohamed M. Morsy[3]

[1] *Graduate Research Assistant, Dept. of Civil and Environmental Engineering, Univ. of Virginia, 351 McCormick Rd., P.O. Box 400742, Charlottesville, VA 22904, jms3fb@virginia.edu*

[2] *Associate Professor, Dept. of Civil and Environmental Engineering, Univ. of Virginia, 351 McCormick Rd., P.O. Box 400742, Charlottesville, VA 22904, goodall@virginia.edu (Corresponding Author)*

[3] *Graduate Research Assistant, Dept. of Civil and Environmental Engineering, Univ. of Virginia, 351 McCormick Rd., P.O. Box 400742, Charlottesville, VA 22904, mmm4dh@virginia.edu; Irrigation and Hydraulics Department, Faculty of Engineering, Cairo University, P.O. Box 12211, Giza 12613, Egypt, mohamedmorsy@eng.cu.edu.eg*

Abstract

In urban areas it is important to have spatially and temporally dense rainfall measurements for flood modeling, monitoring, and prediction. The objective of this paper is to quantify the effect of rain gauge proximity on area-averaged rainfall estimation for small ($<1\text{km}^2$) problematic urban watersheds in Virginia Beach, VA USA. To achieve this, rainfall was estimated by including and then excluding nearby rain gauges from a Kriging analysis. This was done for seven focus watersheds draining to flood prone areas in Virginia Beach for the 20 days with the highest total rainfall depth during the period 07/02/2013 to 01/01/2016. Results show that including local rain gauges in the Kriging analysis resulted in an average percent difference in area-averaged rainfall of close to 60% at a 15-minute time step (24.5 mm max) and 20% at a daily time step (55.6 mm max) across the focus watersheds. The results suggest that a rain gauge within 0.5 km of the target watershed would be needed for flash flood warning applications in Virginia Beach. NEXRAD-derived rainfall estimations were used for comparison and showed significant differences from the rain gauge rainfall estimates greater than 20 mm over an hour (r=0.72, RMSE=9.72 mm)

Introduction

Coastal cities are becoming increasingly vulnerable to flooding (Nicholls and Cazenave, 2010). Recent extreme events, such as hurricanes and tropical storms, have caused severe damage, costing major coastal cities billions of dollars and thousands of lives (Kates et al., 2006; Galarneau et al., 2013). In addition to extreme high return-period events, small return-period rainfall events can also cause flooding in highly urbanized coastal cities and, while less dramatic, these floods can incur significant economic and social costs (Suarez et al., 2005). These lower return-period floods have been occurring more frequently in coastal cities in recent years due to climate change and sea level rise (Ezer and Atkinson, 2014; Sweet et al., 2014). Coastal cities typically have very low topographic relief, large portions of impervious surfaces, a high water table, and tidal influences, which combine to make drainage problematic even without the effects of sea level rise (Titus et al., 1987). Rising sea levels exacerbate drainage problems in coastal cities as tide and groundwater levels rise with the sea level (Bjerklie et al., 2012; Rotzoll and Fletcher, 2012). To add to the flooding problems coastal cities face, precipitation events in general are projected to increase in intensity due to climate change (Alexander et al., 2006; O'Gorman and Schneider, 2009). To understand and accurately forecast flooding in urban, coastal environments, spatially and temporally detailed rainfall data are needed (Smith et al., 2007), but usually unavailable (Hill, 2015). The typical urban watershed is small in area and has a large proportion of impervious surfaces. This results in a short runoff response time, which increases the risk of flash flooding (Hall, 1984; Fletcher et al., 2013).

Often, neither rain gauge networks nor weather radar can provide rainfall measurements at spatial and temporal resolutions needed to make accurate flood forecasts for urban environments (Hill et al., 2014); rain gauge networks are generally too coarse spatially to provide such detailed information (Seo, 1998). The typical weather radar rainfall product has a spatial resolution of 2 km or coarser (Krajewski and Smith, 2002; Nesbitt and Anders, 2009), which may also be too coarse for urban hydrology applications (Smith et al., 2007). Furthermore, weather radar measurements are indirect requiring an empirically-derived relationship between reflectivity and actual rainfall on the ground (Smith and Krajewski, 1993), and is therefore inherently uncertain to some degree. Efforts have been taken to blend rain gauge and weather radar data (Ercan and Goodall, 2013; Velasco-Forero et al., 2009; Seo, 1998; Sun et al., 2000), but spatially detailed and accurate rainfall data often remain a limiting factor in research and flood forecasting (Hill et al., 2014). To increase the spatial coverage of rainfall estimation, less traditional technologies such as measuring signal attenuation between cell phone towers (Overeem et al., 2013; Zinevich et al., 2008) and using simple, more widespread binary rainfall sensors (Hill, 2015) have recently been evaluated, but are still not widely used and, like radar, do not directly measure rainfall.

Although it is generally accepted that spatially and temporally dense measurements are needed to capture storm events relevant to urban hydrology, the degree of spatial and temporal density required is uncertain. Rainfall spatial variability and its effect on hydrology have been studied using both rain gauge networks (Pedersen et al., 2010; Serinaldi, 2008; Jensen and Pedersen, 2005) and weather radar (Krajewski et al., 2003; Smith et al., 2007). Ciach and Krajewski (2006) used 25 rain gauges stations in a 3 km X 3 km grid to observe small-scale spatial and temporal rainfall variation. In their findings, rainfall exhibited high spatial variability with correlation coefficients decreasing between rain gauges at a 4 km separation distance and a 15-minute time step; the correlation coefficients were lower at a 5 minute time step. Emmanuel et al. (2012) analyzed rainfall radar images finding rainfall patterns to be very spatially heterogeneous with decorrelation distances (the distance at which minimal spatial correlation between two points exists) as low as 5 km. Berne et al. (2004) used geostatistics with rain gauge and an X-Band weather radar data to suggest a simple empirical relationship between watershed area and the corresponding necessary temporal resolution of rainfall observations. They then related the temporal resolution to the needed rain gauge spatial resolution. Their findings suggest that watersheds with areas less than 1 km^2 should have rainfall measurements at about a 3 min temporal resolution and a 2.5 km spatial resolution.

The objective of this paper is to quantify the effect of rain gauge proximity on area-averaged rainfall estimation for small (<1 km^2) problematic urban watersheds in a coastal environment using Virginia Beach, VA USA as a case study. Previous studies, as described above, have tended to focus on describing the temporal and spatial characteristics of rainfall generally. This paper adds to the topic by exploring the ability to estimate rainfall for specific urban watersheds with known flooding problems using available rain gauge networks. This paper also presents a general method to determine how proximity of rain gauges to a watershed impacts the areal averaged rainfall estimates for that watershed. First, the station nearest to each focus watershed is removed from the Kriging interpolation routine to measure the difference in area-average rainfall estimated including and then excluding this nearby station. Cheng et al. (2012) also used a method of systematically removing stations from a Kriging rainfall interpolation procedure, but did not focus on quantifying the impact for estimating rainfall over known problem watersheds. Second, the benefit of rain gauge proximity in areal rainfall estimation is further explored by iteratively removing the next nearest rain gauge to the target watershed in the rainfall estimation procedure. This analysis reveals the benefits of having rain gauges within a given distance of the target watershed. Each scenario is conducted for rainfall observations over three different time scales, 15 minutes, hourly, and daily to understand how these time scales factor into the rainfall estimation for the focus watersheds.

The remainder of the paper is organized as follows. First, the methods and data used to assess the effect of rain gauge proximity on flood prone watersheds in Virginia Beach are described. Second, the results are presented and discussed in terms of the benefit of nearby rainfall observations on watershed rainfall estimation. For context, the results are compared to NEXRAD-derived rainfall estimates as an alternative means for generating area-averaged rainfall estimates. Finally, conclusions and recommendations drawn from this study area are given.

Methods

Study Area and Focus Watersheds

Virginia Beach is the most populous city (pop. 450,980) in the Commonwealth of Virginia (U.S. Department of Commerce, 2012). The study area is the most populated portion of Virginia Beach. Shown in Figure 1, it is 370 km^2, 57% of the total city area, and roughly the northern half of the city.

Specific road intersections with recurrent flooding problems were provided by city engineers and public works division employees. The drainage area corresponding to each of these points was delineated using a 1 m by 1 m resolution digital elevation model (DEM). These sub-watersheds are shown in Figure 2 and their characteristics are given in Table 1. For each sub-watershed, the percent imperviousness was obtained from the National Land Cover Dataset 2011 (Homer et al., 2015) and the average slope was calculated from the DEM.

Table 1: Focus watershed areas

ID	Description	Area (km^2)	Imperviousness (%)	Ave. Slope (%)
WS-1	Shore Dr & Great Neck Rd	0.76	59	4.7
WS-2	Shore Dr & Red Tide Rd	0.15	69	0.6
WS-3	Ocean View Ave & Mortons Rd	0.02	43	5.3
WS-4	S. Rosemont & S. Plaza Tr	0.13	61	3.9
WS-5	S. Rosemont & Clubhouse	0.26	26	4.4
WS-6	21st & Baltic	0.08	46	3.3
WS-7	Shore Drive & Kendall St	0.69	9	11

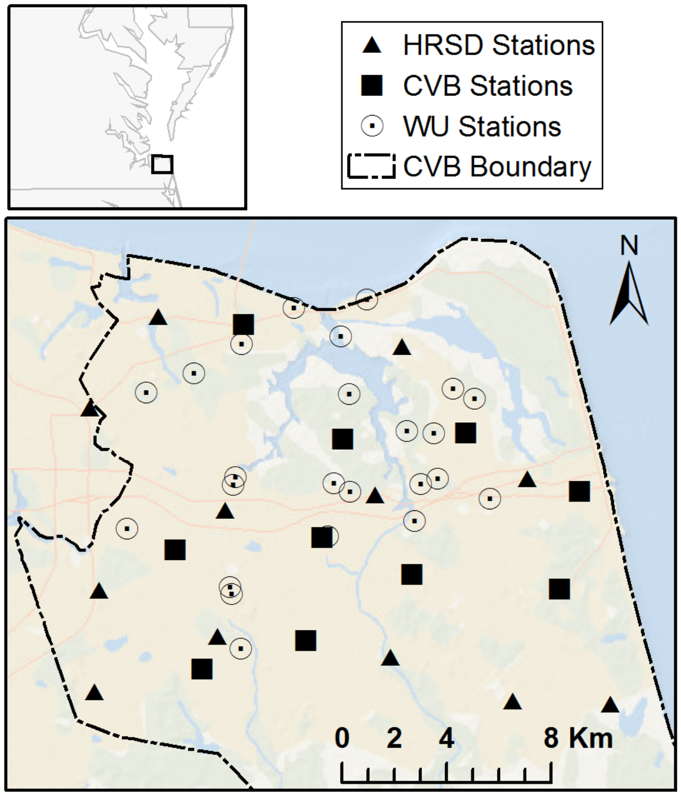

Figure 1: Study area, the northern portion of Virginia Beach.

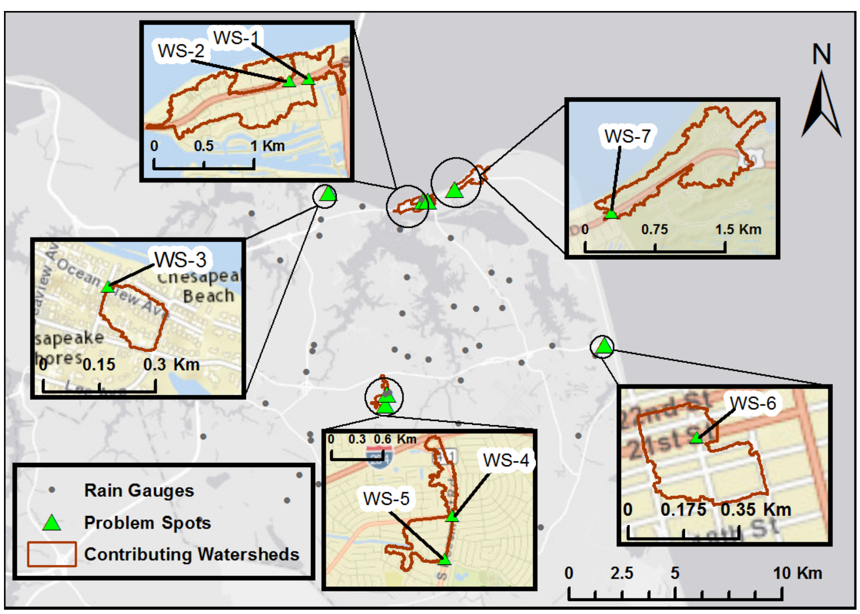

Figure 2: Focus watersheds which drain into known flood prone locations.

Rainfall Data

Rainfall data measured at the Oceana Naval Air Station were used to select focus dates for the analysis. The Oceana Naval Air Station rain gauge was used to select the dates because it is the only weather station run by the U.S. National Weather Service located within the study area. The 20 days with the highest daily accumulated rainfall at the Oceana Naval Air Station were selected as focus dates for the analysis. For these dates, precipitation data were obtained from three different sources: The City of Virginia Beach, Hampton Roads Sanitation District, and Weather Underground. Figure 3 shows the daily rainfall totals averaged over all of the rain gauges from the three data sources for the 20 focus dates. The standard deviations of these averages are also shown to demonstrate the range in rainfall variability in the 20 days analyzed.

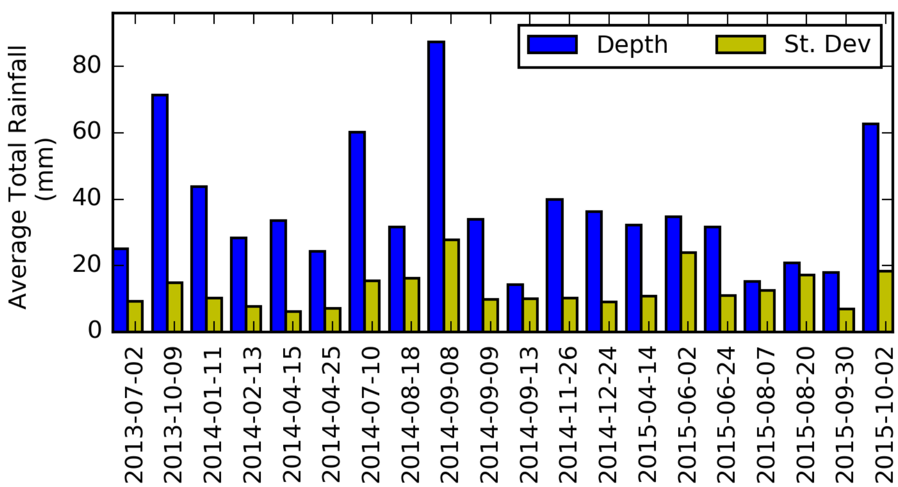

Figure 3: Total daily rainfall averaged over all rain gauges for focus dates

The City of Virginia Beach (CVB) in the past five years has installed a rain gauge network consisting of 14 stations. Precipitation data from the 10 gauges within the study area were obtained for the 20 days analyzed. The Hampton Roads Sanitation District (HRSD) has a network of over 50 rain gauges in the Hampton Roads region, 12 of which are within the study region. The data from these 12 gauges, which are quality controlled by the HRSD, were also obtained for the 20 days analyzed. Rainfall data were also obtained from Weather Underground (WU) (http://www.wunderground.com/). WU includes more than 100,000 personal weather stations, purchased and maintained by with their data accessible through the WU site. There were between 7 and 21 WU personal weather stations that reported rainfall values in the study area for the 20 days examined; that corresponds to a 32-

95% increase in the number of rain gauges in the study area. Increased spatial coverage has obvious benefits in better understanding spatially heterogeneous precipitation events. However, the data are collected by individual citizen scientists without a quality controlling standard, therefore the validity of the data is uncertain. The process for screening this dataset to identify invalid observations is described in the following section.

Rainfall data from the three sources, CVB, HRSD, and WU, were observed at different temporal resolutions. CVB and HRSD had measurement intervals of 5 and 15 minutes, respectively. Because the WU rain gauges are owned by individuals, the temporal resolution of measurements at these stations varied with an average of 6.2 minutes between observations. Three temporal resolutions were used for the analysis: daily, hourly, and 15 minute. The finest resolution used in the analysis was the coarsest of the three sources: 15 minutes from the HRSD data. The measurements at a temporal resolution finer than 15 minutes were aggregated so that all of the measurements were on a consistent same time scale. The measurements were also aggregated to hourly and daily time scales to study the effect of the time scale on area-averaged rainfall estimation.

Analysis

Quality Controlling of Rainfall Data

The rainfall data from all three data sources were quality controlled first to identify stations not functioning properly on the focus dates. If a station recorded a daily rainfall total of zero for any of the 20 days analyzed, it was assumed that the station was not functioning properly and all values from that station that day, were disregarded. Given that these were the 20 days with the greatest total rainfall over the period of analysis, if a rain gauge did not record any rainfall it was assumed that the rain gauge was not working on that day.

Because the WU data were considered to be less reliable for the reasons described above, these data underwent a simple quality control procedure to identify potentially errant measurements on a 15-minute time scale. At each station, inverse distance weighting (IDW) was used to predict the rainfall based on recorded values from its neighboring CVB and HRSD stations. A minimum of three CVB and HRSD stations, all within 5 km, were used for the estimation. For each 15-minute time step, the IDW estimated value was compared to the value recorded at the WU station in question. If the difference between the predicted value and the recorded value was greater than three times the standard deviation of the measurements used for the IDW prediction, then that measurement was flagged as an outlier. The measurement was also flagged as an outlier if the IDW predicted value was greater than 10 mm and the recorded value was zero. This was to check for stations being off-line intermittently during the focus dates.

The quality control procedure described above was also performed for the CVB and HRSD stations. The number of outliers found from the CVB and HRSD stations served as a baseline against which to compare the number of outliers recorded by the WU stations. If the number of outliers recorded by a WU station was significantly higher than the number recorded by the CVB and HRSD stations, it was judged that the outlying measurements recorded were not the result of real spatial variation, but were the result of measurement errors. The data from the station were therefore disregarded.

Rainfall Interpolation using Kriging

Ordinary Kriging, which assumes a constant, unknown mean over the search neighborhood, was used to quantify the importance of rain gauge proximity in estimating rainfall depth over the seven focus watersheds. It would have been preferable to use Kriging with external drift (Kebaili Bargaoui and Chebbi, 2009); however, this technique requires another related but independent variable such as elevation (Goovaerts, 2000). In this case, since the study area is located near the coastal plane, its elevation is effectively constant. A spherical model was used (Equation 1) for the Kriging semi-variogram models where γ is the variogram, h is the lag, c is the sill, and a is the range. The semi-variograms were assumed to be isotropic. The model parameters (sill and range) were automatically optimized using the RGeostats package (Renard et al., 2015) in R and were calculated for each individual time step with all available data. The Kriging process produced two outputs: the predicted rainfall and the Kriging variance. Kriging variance is the variance of the predicted rainfall value and is a measure of prediction confidence. Both of these outputs were produced as continuous raster datasets and their values were averaged over the area of the focus watersheds to obtain area-averaged estimates of rainfall and Kriging variance using the ArcGIS's Zonal Statistics as Table tool.

$$\gamma(h) = \begin{cases} c\left[\frac{3}{2}\frac{h}{a} - \frac{1}{2}\left(\frac{h}{a}\right)^3\right] & \text{if } h \leq a \\ c & \text{otherwise} \end{cases} \tag{1}$$

Experiment 1: Removing the Nearest Stations to a Watershed To quantify the role of nearby rain gauge stations in area-averaged precipitation estimates for the seven focus watersheds, the rainfall was estimated with and then without the nearest quality controlled (from HRSD or CVB) rain gauge station. Any WU rain gauges closer than the nearest quality controlled rain gauge were also removed. For example, considering the watershed diagram in Figure 4; S_2 would be excluded, being the closest quality controlled station, and S_1 would also be removed because it is a WU station closer to the watershed centroid than S_2. The number of rain gauges removed for each focus watershed and the average distance of the removed rain gauges are shown in Table 2. The table also gives distances for the next nearest station that was not removed in the analysis (i.e., S_3 in Figure 4).

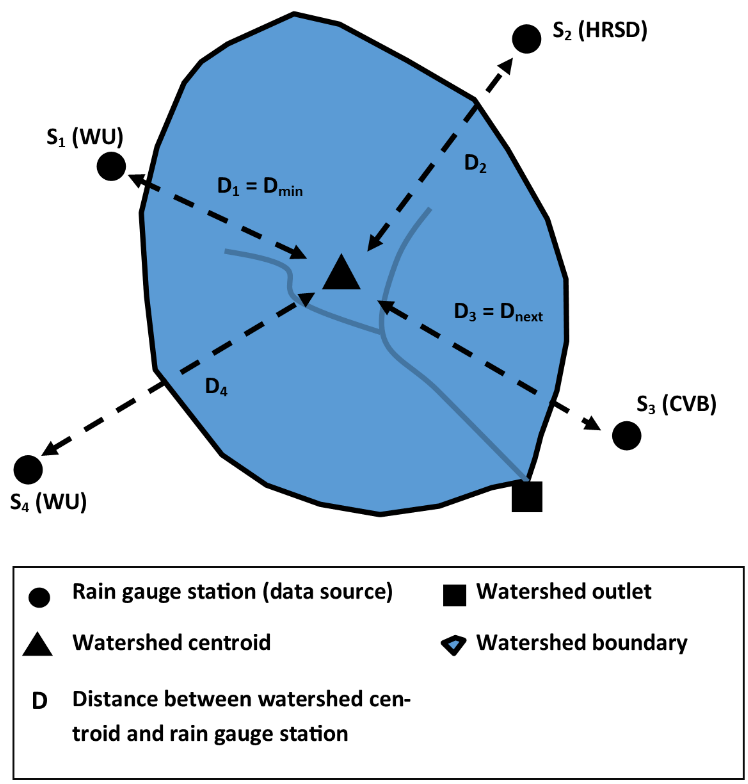

Figure 4: Diagram illustrating two Kriging experiments

Table 2: Gauges removed in Experiment 1. Distances are measured from watershed centroid.

ID	Num.gauges removed	Distances of removed gauges (m)	Distance to next nearest station (m)
WS-1	3	318, 1419, 2288	2518
WS-2	3	153, 1624, 2340	2643
WS-3	1	1266	1605
WS-4	2	458, 466	1671
WS-5	2	380, 542	2414
WS-6	1	625	2449
WS-7	2	2645, 3016	4201

Two variables were calculated to quantify the impact of removing the nearby stations on rainfall estimates. The first variable is the average increase in variance ($\overline{\Delta\mathrm{Var}}_i$) and the second variable is the average absolute difference in rainfall estimation ($|\overline{\Delta\mathrm{R}}_i|$). These variables were calculated using Equations 2 and 3, respectively. In Equation 2, $\mathrm{Var}_i(t)'$ is calculated the same way as $\mathrm{Var}_i(t)$, the variance of the estimated rainfall on watershed i at time t, but it is calculated without the nearby station(s). Similarly $R_i(t)'$ in Equation 3 is calculated in the same was as $R_i(t)$, the estimated rainfall on watershed i at time t, but without the nearest station(s). As shown in the equations, the difference between $\mathrm{Var}_i(t)'$ and $\mathrm{Var}_i(t)$, and $R_i(t)'$ and $R_i(t)$ is averaged over all values in the time series, $t = 0, ..., N$. Equations 2 and 3 were applied to each of the three time scales considered in the analysis: 15-minute, hourly, and daily.

$$\overline{\Delta\mathrm{Var}}_i = \frac{1}{N}\sum_{t=0}^{N} \frac{\mathrm{Var}_i(t)' - \mathrm{Var}_i(t)}{\mathrm{Var}_i(t)} \tag{2}$$

$$|\overline{\Delta\mathrm{R}}_i| = \frac{1}{N}\sum_{t=0}^{N} \left| \frac{R_i(t)' - R_i(t)}{(R_i(t)' + R_i(t))/2} \right| \tag{3}$$

Experiment 2: Removing Stations at Increasing Distances from a Watershed A second experiment was performed to quantify the effect of excluding rain gauge stations, at increasing distances from a watershed, on rainfall estimation for that watershed. For each focus watershed, the nearest rain gauge to the watershed centroid was excluded from the rainfall estimation. Unlike Experiment 1, there was no distinction made between stations from different sources in Experiment 2. After the nearest station was excluded, the two nearest stations were excluded from the rainfall estimation. This was repeated until all rain gauges within 8 km of the watershed centroid were excluded. Note that the the cases in Experiment 1 are also contained in Experiment 2. Experiment 2, therefore, can be thought of as an extension of Experiment 1. Similar to Experiment 1, in Experiment 2 the average increase in variance ($\overline{\Delta\mathrm{Var}}_i$) and the average absolute difference in rainfall estimation ($|\overline{\Delta\mathrm{R}}_i|$) were calculated for the seven watersheds and the three time scales. However, while in Experiment 1 Equations 2 and 3 were applied using all stations in the study area, in Experiment 2 these equations were applied using only a subset of the stations in the study area, i.e. with removing individual stations up to 8 km from the watershed centroids as explained above.

Comparison with Weather Radar Data

Given that dense rain gauge networks are rare, and that weather radar products are much more widespread (the vast majority of the continental United States is covered by NEXRAD radars), the results of the analysis were compared to weather radar-derived rainfall estimates. The weather radar data used for the comparison was the NEXRAD Level III product "DAA," which is the one-hour precipitation accumulation estimation produced using the Quantitative Precipitation Estimate (QPE) dual-polarization precipitation algorithm which has 256 possible data levels (NOAA, 2017). This product was selected instead of the one-hour precipitation accumulation calculated using Precipitation Processing System (PPS) based on results from Wu et al. (2012) who found QPE to be generally more reliable than PPS. The spatial resolution of the data was 0.24 km x 1.5 km grid. The NEXRAD data were obtained for each hour of the 20 days analyzed and converted from native binary to a Geotiff raster format using the NOAA Weather and Climate Toolkit. The Zonal Statistics as Table tool in ArcGIS was then used to obtain the average value of the NEXRAD raster cells that intersected each watershed. These area-averaged estimates were compared with the area-averaged estimates obtained from the Kriging of the rain gauge data.

Results and Discussion

Quality Controlling Results

Results from the quality control showed that 8 of the total 44 stations recorded zero rainfall for at least 12 of the 20 days analyzed (Table 3); 6 of these 8 stations were WU stations and 2 were HRSD stations. WU station "KVAVIRGI105" had the most occurrences with 8 of the 20 days reporting zero rainfall. Stations were excluded from the analysis for the day(s) that zero rainfall was reported. It is possible that one rain gauge in such a large area would have had no rainfall even when most rain gauges did. That said, on 8 of the 12 days on which zero rainfall was recorded somewhere in the study area, zero rainfall was only reported at one rain gauge for the day. Since every other rain gauge was reporting at least some rainfall for each of those 8 days, it was assumed that the one that recorded zero rainfall was not functioning. On 3 of the 12 days, 2 stations reported zero rainfall, and on 1 day (2015-09-30) 4 stations recorded zero rainfall. In these cases, since no two stations closest to each other both reported zero rainfall, these stations were also assumed to be not functioning.

The results of the quality control procedure used to identify anomalous measurements from the

Table 3: Stations and dates where a value of zero rainfall was recorded

StationID	Source	Zero-sum Dates
KVAVIRGI71	WU	2014-09-13
KVAVIRGI79	WU	2014-09-13
KVAVIRGI88	WU	2015-09-30, 2015-10-02
KVAVIRGI105	WU	2014-11-26, 2015-04-14, 2015-06-02, 2015-08-07, 2015-08,02, 2015-09-30, 2015-10-02
KVAVIRGI116	WU	2015-09-30
KVAVIRGI65	WU	2015-09-30
MMPS-036	HRSD	2014-08-18, 2014-09-08, 2014-09-09
MMPS-160	HRSD	2014-04-14

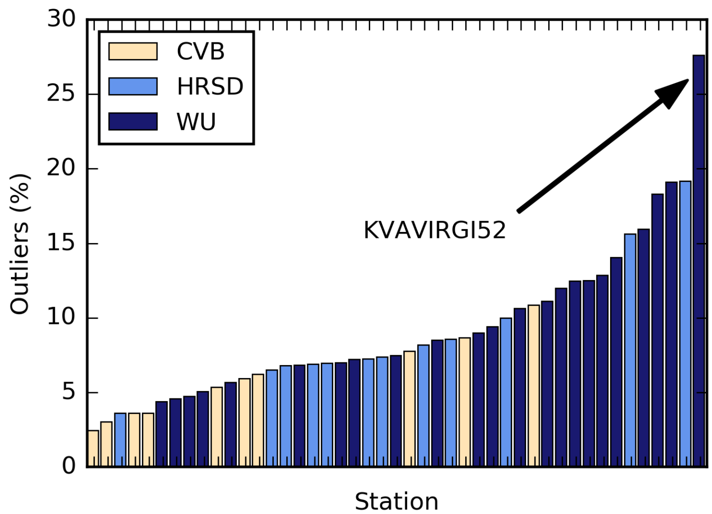

Figure 5: Percent of outliers for each station

Table 4: Percentage of outliers for each data source

Data Source	Average Percentage of Outliers (%)
CVB	4.5
HRSD	6.9
WU	8.6

stations are shown in Figure 5. From a total of 31,095 observations, 2,045 were identified as outliers. More than 99% of the outliers identified were three or more standard deviations away from the estimate based on their neighbors, compared to less than 1% which were recorded as zero when the IDW estimate was 10 mm or greater. Eight of the top ten stations in terms of percentage of outliers were WU stations. The WU stations had a higher average percentage of outliers overall (Table 4). Only one station stood out statistically: “KVAVIRGI52”. The percentage of measurements classified as outliers from this station was 3.6 standard deviations from the mean percent number of observations classified as outliers when considering all stations. “KVAVIRGI52” was therefore excluded from the analysis, while all other stations were kept.

Exploratory Analysis Results

Figure 6 shows the daily rainfall depths for each station across the study area. There are clear differences in rainfall magnitude and spatial variation between dates. For example, considering the daily total rainfall values for 2014-12-24, 2015-04-14, 2015-06-02, and 2015-06-24, it is clear visually that the daily rainfall on 2015-06-02 is more spatially heterogeneous than the other dates. The data in Table 6 confirm this quantitatively. These four daily totals are quite similar: 36.2, 32.6, 34.3, and 31.8 mm, respectively. However, their standard deviations are more variable: 8.9, 11.0, 23.9, and 10.8 mm, respectively. The spatial variation seen visually in Figure 6 maybe best be explained quantitatively by the standard deviation to mean ratio, or coefficient of variation (CV). Contrasting the plots of the two dates with the lowest CV, 2014-04-15 (0.18), and the highest CV, 2015-08-20 (0.85), the spatial uniformity on 2014-04-15 and the spatial non-uniformity on 2015-08-20 are clearly seen (Table 6).

Although the rainfall can be relatively spatially uniform for a given day, when considering a shorter time step, the spatial variation is often much higher. This can be seen in the 15-minute and hourly CVs which are, on average, at least four times higher than the daily CV (Table 5). Even the date with the smallest daily CV, 2014-04-15 (0.18), shows considerable variability in rainfall amounts across stations at the 15-min time step (CV up to 0.65 at 11:15:00; Figure 7). This variability on smaller time steps is important to consider for flood forecasting applications in small, highly impervious watersheds with flashy responses. The uncertainty caused by this variation could result in inaccurate predictions about the potential for flooding risk.

Table 5: Average CV for the time steps examined

Time scale	Average CV
15 minute	2.1
Hourly	2.0
Daily	0.5

Experiment 1 Results

The results of the rainfall estimation without local information are summarized in Figure 8. For most of the watersheds, the variance increased by more than 100% and, generally, the magnitude of

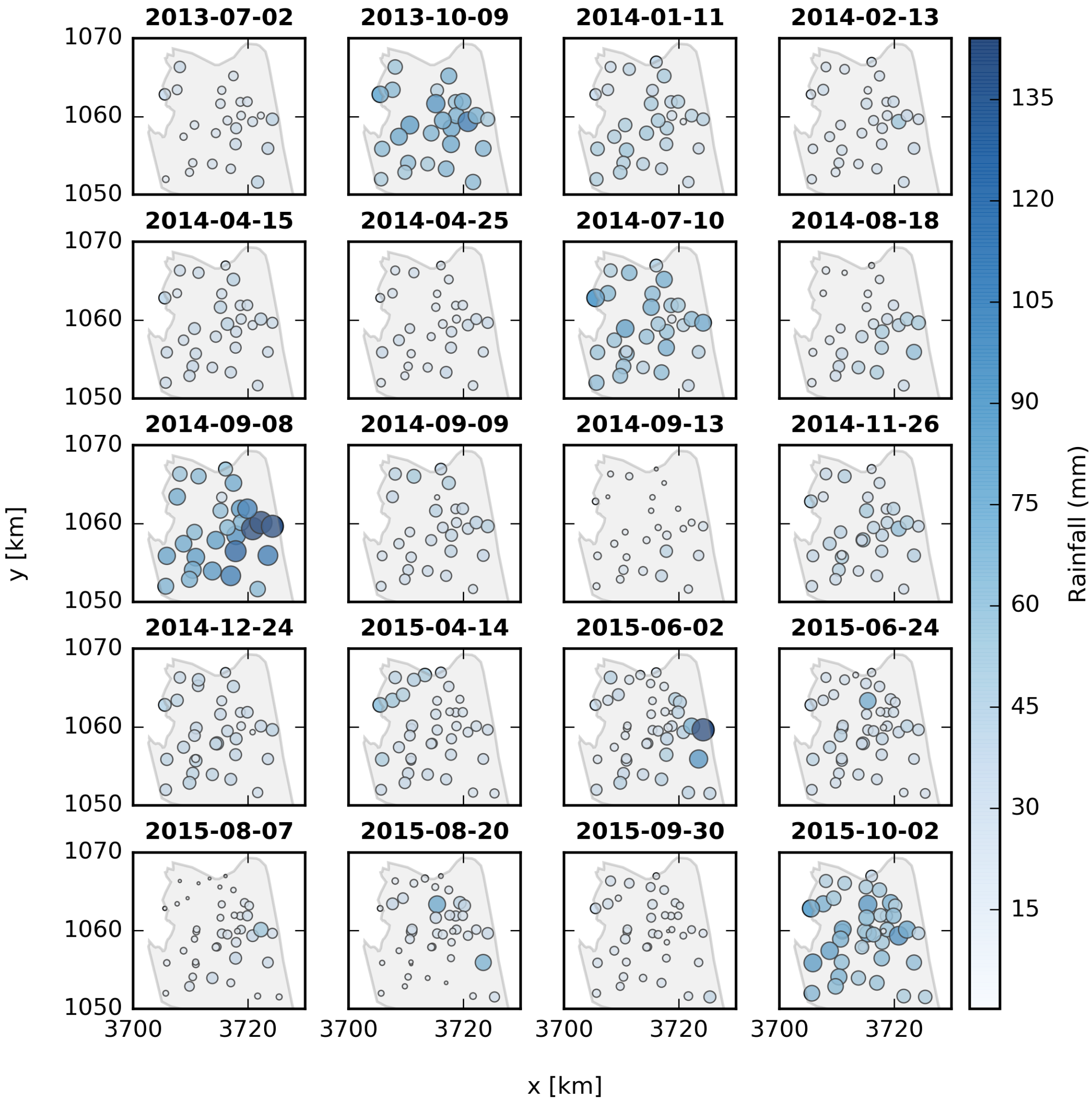

Figure 6: Daily rainfall values at each station (size of the scatter points corresponds to relative magnitude of rainfall)

the increase corresponded to the distance from the watershed centroid to the nearest excluded rain gauge station (see Table 2). For example, the watersheds that had the greatest distance from their centroid to the nearest rain gauge, WS-7 (2645 m) and WS-3 (1266 m), had the smallest increase in variance when those rain gauges are removed. Conversely, the watershed that had the smallest distance between its centroid and the closest rain gauge, WS-2 (153 m), had the largest increase in

Table 6: Summary data for daily rainfall

Date	Mean (mm)	Standard Dev. (mm)	CV
2013-07-02	25.1	9.2	0.36
2013-10-09	68.8	19.9	0.29
2014-01-11	43.7	10.1	0.23
2014-02-13	28.0	7.7	0.28
2014-04-15	33.5	6.1	0.18
2014-04-25	24.2	7.1	0.29
2014-07-10	58.5	18.1	0.31
2014-08-18	31.6	16.3	0.51
2014-09-08	84.7	30.9	0.36
2014-09-09	33.1	10.5	0.32
2014-09-13	13.8	10.1	0.73
2014-11-26	39.3	10.6	0.27
2014-12-24	36.2	8.9	0.25
2015-04-14	32.6	11.0	0.34
2015-06-02	34.3	23.9	0.70
2015-06-24	31.8	10.8	0.34
2015-08-07	15.0	12.4	0.82
2015-08-20	20.4	17.3	0.85
2015-09-30	17.8	6.9	0.39
2015-10-02	61.5	19.8	0.32

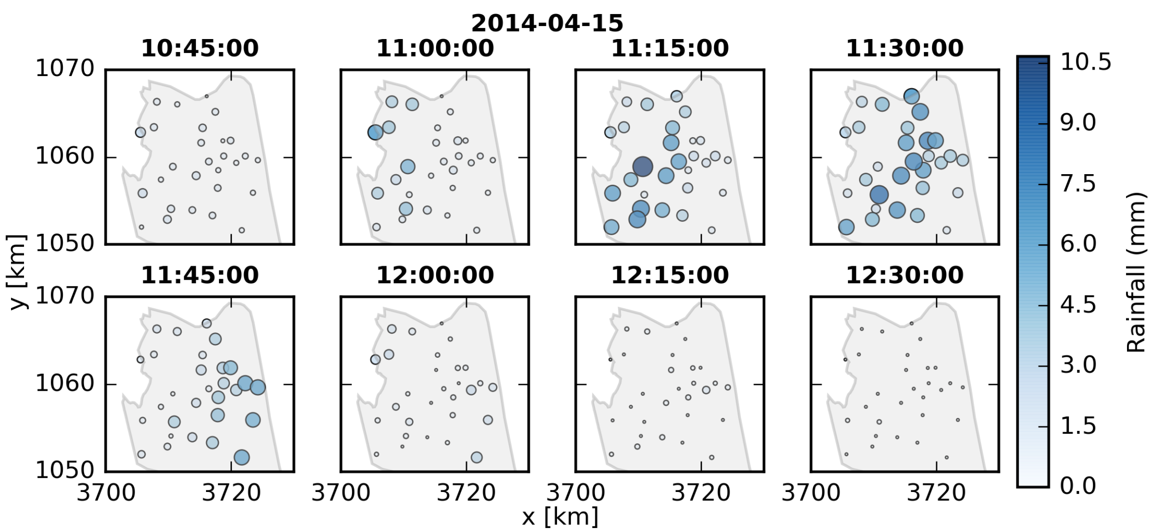

Figure 7: 15-min rainfall values for 2014-04-15, a storm with low daily spatial variability (size of the scatter points corresponds to relative magnitude of rainfall).

variance when that rain gauge was removed. For the most part, these values vary little between the three time scales (15 min, hourly, and daily). This is because the variance is related more to the spatial arrangement of the observations than their actual magnitude.

Figure 8 shows the average absolute difference in rainfall estimation when the nearby stations are

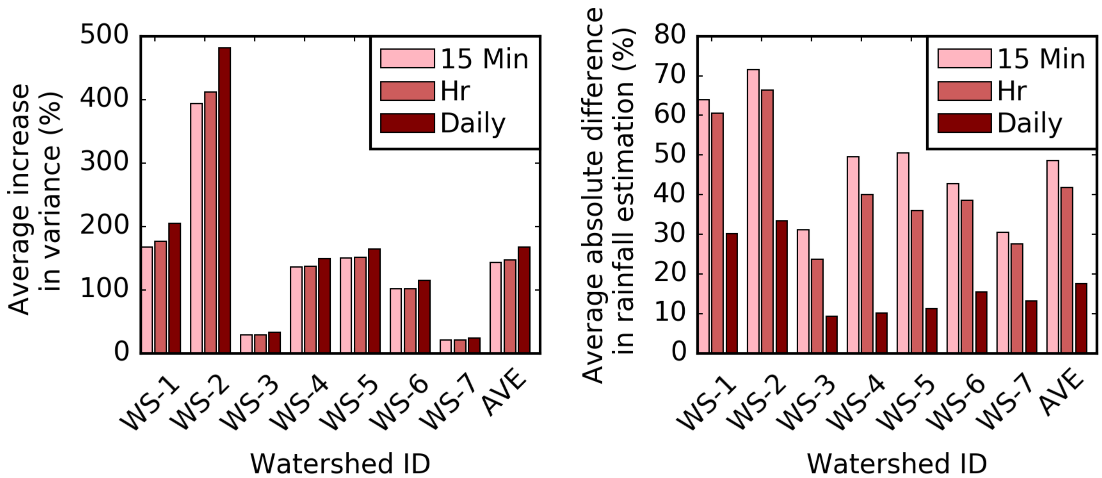

Figure 8: Average percent increase in variance and percent difference in rainfall estimation without nearest stations (Experiment 1)

excluded. On average, the percent difference in rainfall estimation for the 15-minute time step was 49% with a maximum of 72% for WS-2. The average absolute difference in rainfall estimation at the 15-minute time step was 0.34 mm. For 15-minute intervals with more rainfall recorded, the difference was generally larger. Figure 9 shows a histogram of the absolute difference in rainfall estimation at the 15-minute time step when the rainfall estimated including the nearest rain gauge was above 5 mm. Out of the 155 data points, 16 had differences greater than 5 mm. The maximum difference in rainfall estimation was 24.5 mm at WS-6, which occurred on 2015-06-02. Without the nearest rain gauge, the estimated rainfall was 7.4 mm; with the nearest rain gauge included, the rainfall estimate was 31.9 mm. For perspective, this difference can be thought of in terms of design storms. The estimated rainfall intensity including the nearby rain gauge (31.9 mm/15 min or 128 mm/hr) for this 15-minute time period corresponded to a 10-year, 15-minute design storm. If this station did not exist, the estimated rainfall intensity (7.4 mm/15 min or 29.6 mm/hr) would erroneously be considered negligible by design standards (Bonnin et al., 2006).

The results from Experiment 1 were used to compare the distances between rain gauges and the focus watersheds, to the rain gauge distance recommendations made by Berne et al. (Table 7). Berne et al. analyzed radar and rain gauge data to recommend temporal and spatial resolution requirements for urban watersheds based on the watershed surface area. Table 2 lists the distances of removed rain gauges and Table 7 lists the recommended distances for the seven focus watersheds based on their surface area. Four of the seven focus watersheds in this study had more than one rain gauge station

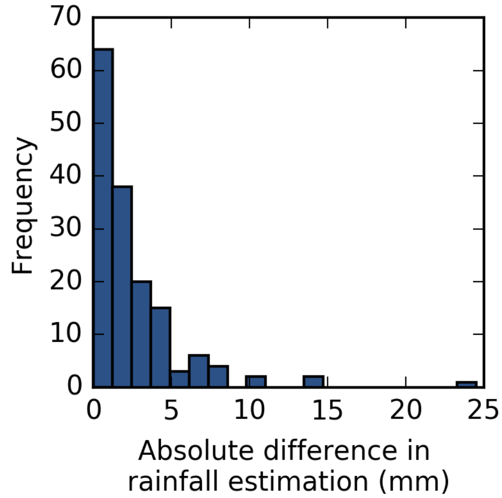

Figure 9: Histogram of absolute differences in rainfall estimation in Experiment 1 when rainfall estimates including the nearest gauge were greater than 5 mm

within the distance recommended by Berne et al.: WS-1, WS-2, WS-4, WS-5. When the closest rain gauge was removed, the average rainfall estimation changed significantly for each watershed at the 15-minute scale (49%, 60%, 37%, and 44%, respectively). One would expect the difference in rainfall estimation to be much smaller given that one rain gauge station was still within the recommended distance. This suggests that the recommended distances offered by Berne et al. would be too coarse for the study area. The difference in results obtained in this study and Berne et al's may be due to climatic or geographic differences between the study area an urban area on the East Coast of the U.S., and the one used by Berne et al. (2004), a coastal. area in Southern France.

Table 7: Experiment 1 results compared to literature-recommended spatial resolutions

ID	Recommended distance to rain gauge (Berne et al., 2004))(km)	Ave. difference at 15 min time scale when nearest rain gauge within the recommended distance is removed
WS-1	2.5	49%
WS-2	2.0	60%
WS-3	1.4	NA
WS-4	1.9	37%
WS-5	2.1	44%
WS-6	1.8	NA
WS-7	2.5	NA

Experiment 2 Results

Results from Experiment 2 show the impact that removing rain gauges at increasing distances from a focus watershed has on rainfall estimation for that focus watershed. Figure 10 shows how variance changes when increasing the distance of removed stations from watershed centroids. The change in variance decreases drastically as the distance increases from 0 to 1.5 km, and is effectively negligible by 3.5 km. The greatest change in these results occurs within 1 km. Therefore, on average in this study area, to appreciably increase the confidence of rainfall estimation, a new rain gauge must be within 3.5 km of a given watershed's centroid and would preferably be within 0.5 km.

Figure 11 shows how the rainfall estimation changes for each focus watershed as stations are excluded from the Kriging analysis. A linear model was fit to the data for each watershed. For all but WS-4 and WS-5, the R^2 values were at least 0.72, suggesting a linear relationship between distance to the furthest removed rain gauge and the percent change in rainfall estimation for these watersheds.

There may be several reasons why the relationship between distance to the furthest removed rain gauge and the percent change in rainfall estimation for WS-4 and WS-5 appears to be non-linear. One possible explanation is the geography of the watersheds. WS-4 and WS-5 are located more inland compared to the other watersheds. Rainfall variation corresponding to distance from the coast has been previously observed elsewhere (Hayward and Clarke, 1996). The spatial relationship of the neighboring rain gauges may also be a factor. Since WS-4 and WS-5 are located in the center of the rain gauge network, the rain gauges were removed in the analysis from all sides of the watersheds. In contrast, because the other watersheds were on the coast, the rain gauges removed for these watersheds were only from the inland side. Further research specifying the direction from which rain gauges are removed in the analysis would help test this explanation.

Comparison with Weather Radar Data Results

Figure 12 shows the results of the comparison between the area-averaged rainfall estimates based on the Kriging analysis using the rain gauge data, and the area-averaged rainfall estimates from the NEXRAD DAA data. The figure reports the root mean squared error and Pearson correlation coefficient ("RMSE" and "r" on the figure, respectively). The Figure 12a-12g show the comparison of the estimates from the two data sources for each of the seven focus watersheds. For these comparisons, the correlation coefficients were between 0.87 and 0.94. Similarly, the RMSE values were between 2.70 mm and 3.71 mm. Many of the hourly rainfall estimates are small (less than 10 mm) and thus would

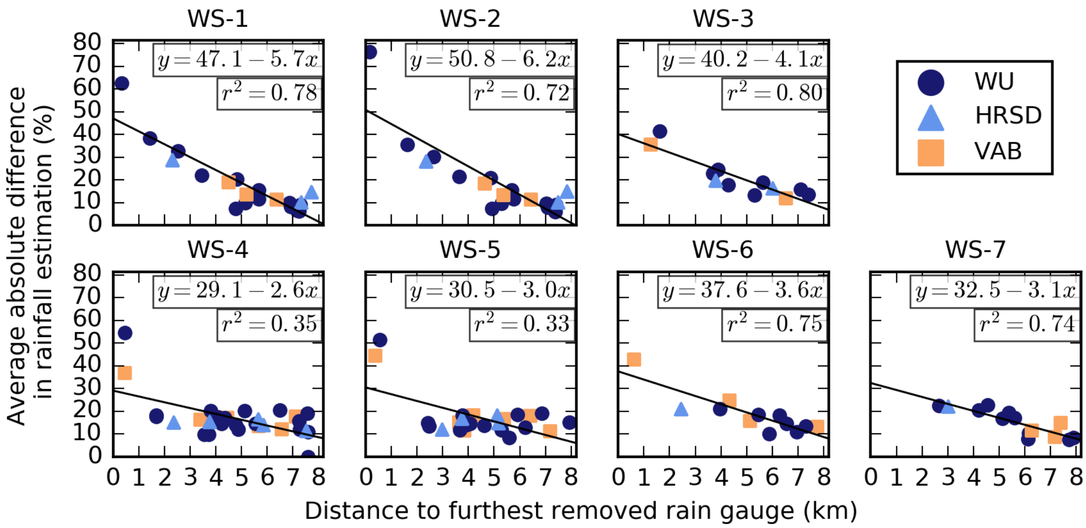

Figure 10: Percent increase in variance compared to distance from watershed centroid to excluded measurement stations at 15-minute time scale (Experiment 2)

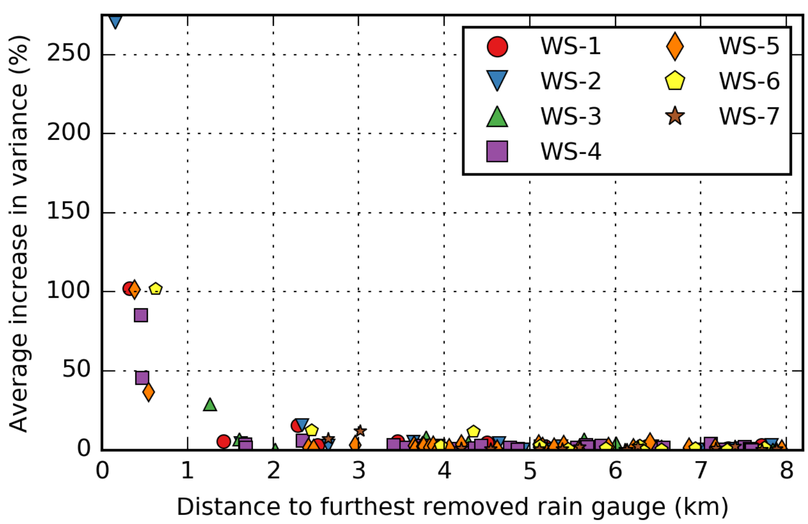

Figure 11: Percent difference in rainfall estimations compared to distance from watershed centroid to excluded measurement stations at 15-minute time scale (Experiment 2)

probably not contribute to flooding. To focus on rainfall totals more likely to contribute to flooding, the rainfall estimates greater than 20 mm (based on the rain gauge-based estimate) for all of the focus watersheds were calculated (Figure 12h). This subset of the data is much more scattered with a correlation coefficient of 0.72 and a RMSE of 9.72 mm. The increased scatter for large rainfall magnitudes, their coarse temporal (minimum 1 hr) and spatial resolution (1.5 km) limits the ability of NEXRAD DAA rainfall product in urban flash flood applications in this study area.

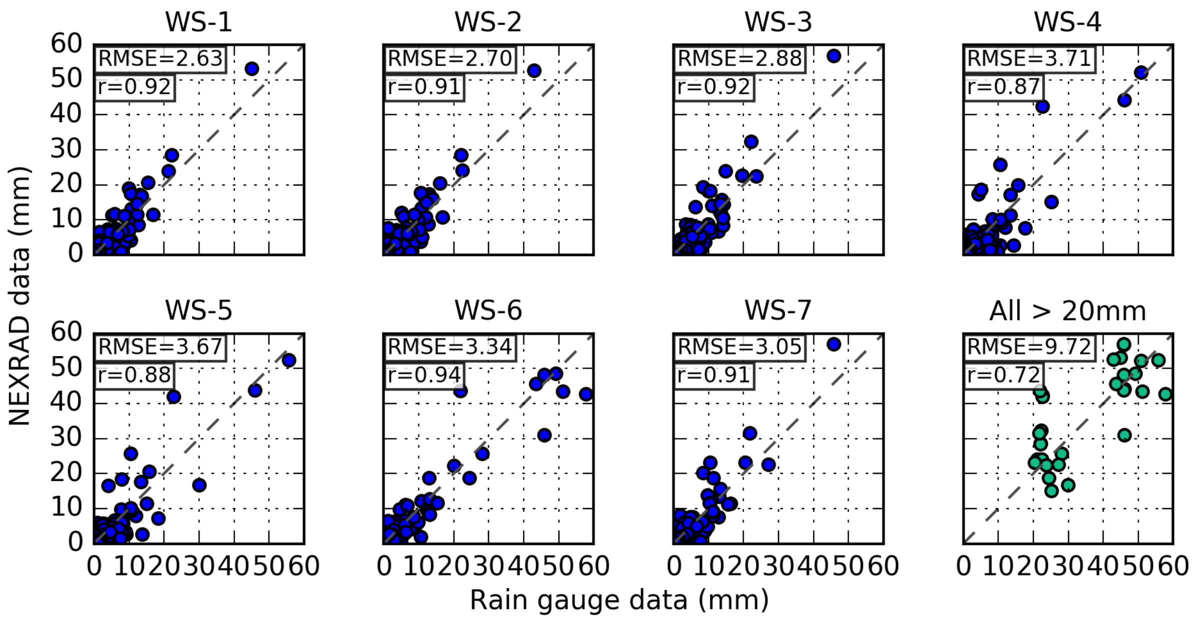

Figure 12: Comparison of area-averaged rainfall estimation based on the Kriging of rain gauge data and area-averaged NEXRAD DAA product data. The first seven subplots compare all of estimates by focus watershed. The last subplot (lower right-most) shows the comparison of the rainfall estimates greater than 20 mm (based on the rain gauge estimates) from all focus watersheds.

Conclusions

The objective of this paper is to quantify the effect of rain gauge proximity on area-averaged rainfall estimation for small (<1 km^2) problematic urban watersheds. Virginia Beach, VA. served as the case study for the analysis. Rainfall data from three different sources, the City of Virginia Beach (CVB), the Hampton Roads Sanitation District (HRSD), and Weather Underground (WU), were collected. In total, rainfall data from 44 stations for the 20 days with the highest rainfall totals over a three year period were used in the analysis. The WU data were quality controlled on a station by station basis resulting in one station being excluded from the analysis. Kriging was performed to quantify the effect of nearby stations on the rainfall estimation for seven focus sub-watersheds. The results were then compared to radar rainfall estimates for context.

The nearest quality controlled rain gauge to the focus watershed centroids and all closer rain gauges were removed from the network to understand the effect of nearby rain gauges on rainfall estimation. The results of this analysis indicate that rainfall estimations change on average by about 50% across all the watersheds at a 15-minute time step when the nearest station is excluded. For a single watershed, the highest average change in rainfall estimation was over 70% at a 15-minute time step with the largest difference in rainfall estimation of 24.5 mm at a 15-minute time step. This corresponds to the difference between a negligible design storm and a 10-year, 15-minute design storm. Differences of this magnitude could drastically affect flood forecast applications for these small, flashy, urban watersheds.

An analysis was also performed to assess the effect on rainfall estimation and variance from increasingly distant rain gauges to the watershed centroid. The results suggest that rain gauges added within 0.5 km can decrease variance by 50-100% and a rain gauge 3.5 km from the watershed centroid will not decrease estimation variance appreciably. The current rain gauge network has stations within 0.5 km for four of the seven focus watersheds. As flooding problems continue to increase within coastal regions due to climate change and sea level rise, additional problem areas are likely to arise.

To put the analysis of the rain gauge data in the context of radar-derived rainfall products, the rainfall estimation based on a Kriging analysis using the rain gauge data was compared with NEXRAD-derived rainfall estimations. This comparison was on an hourly time step, the finest temporal resolution of the NEXRAD Level III rainfall estimation products. When considering all magnitudes of rainfall estimation, the correlation between the two sources was high (correlation coefficients between 0.87 and 0.94, RMSE between 2.70 mm and 3.71 mm). However, when considering only the higher magnitude estimates more likely to cause flooding (greater than 20 mm) the correlation decreased (correlation coefficient of 0.72, RMSE of 9.72 mm). Besides the decreased correlation with greater rainfall, the unavailability of NEXRAD Level III products at a sub-hourly temporal resolution and coarse spatial resolution of the data (cell sizes of roughly 0.25 km x 1.5 km for the study area) limit current NEXRAD-derived Level III rainfall products in this area for flash-flood applications.

If the long term goal were to cover the entire study area with regularly spaced rain gauges at a 1 km spacing, so that every point would be roughly within 0.5 km of a rain gauge, then 471 stations would be required. Recognizing that this is impractical with existing technology, alternatives could be explored to obtain the dense rainfall data needed to predict flash flooding in an urban setting. An obvious alternative is to focus resources by deploying rain gauges near problem areas. For the current study area, this could begin with adding rain gauges within 0.5 km of the three focus watersheds which do not currently have a rain gauge within that distance. A longer term option may be to refine the use of and advance weather radar technology, specifically focused for fine temporal and spatial resolutions required for urban flash flood warning. Also, advancements in sensor and information technology will also play a role in making denser rainfall networks possible. For example, using acoustic rain gauges, that, unlike the more common tipping bucket rain gauge, do not contain moving parts may reduce costs allowing for larger deployments. Cheaper, binary rainfall sensors could also help fill the need of dense rainfall measurements (Hill, 2015). Leveraging larger efforts like the Internet of Things (IoT) technologies and cyber-physical systems (CPS) approaches, will make it possible to glean meaningful information from observations, and to use this information in stormwater infrastructure controls such as valves, storm gates, and pumps to create a smarter storm water management systems for flood mitigation.

Acknowledgments

The authors thank the City of Virginia Beach, the Hampton Roads Sanitation District, and Weather Underground for the access to their rainfall data. The authors also acknowledge funding provided by the Mid-Atlantic Transportation Sustainability Center University Transportation Center.

References

Alexander, L. V., Zhang, X., Peterson, T. C., Caesar, J., Gleason, B., Klein Tank, A. M. G., Haylock, M., Collins, D., Trewin, B., Rahimzadeh, F., Tagipour, A., Rupa Kumar, K., Revadekar, J., Griffiths, G., Vincent, L., Stephenson, D. B., Burn, J., Aguilar, E., Brunet, M., Taylor, M., New, M., Zhai, P., Rusticucci, M., and Vazquez-Aguirre, J. L. (2006). Global observed changes in daily climate extremes of temperature and precipitation. *Journal of Geophysical Research*, 111(D5):D05109.

Berne, A., Delrieu, G., Creutin, J. D., and Obled, C. (2004). Temporal and spatial resolution of rainfall measurements required for urban hydrology. *Journal of Hydrology*, 299(3-4):166–179.

Bjerklie, D. M., Mullaney, J. R., Stone, J. R., Skinner, B. J., and Ramlow, M. A. (2012). Preliminary investigation of the effects of sea-level rise on groundwater levels in New Haven, Connecticut. *Open-File Report*, Open-File Report 2012-1025, US Geological Survey. https://pubs.er.usgs.gov/publication/ofr20121025. Accessed Aug 2016.

Bonnin, G. M., Martin, D., Lin, B., Parzybok, T., Yekta, M., and Riley, D. (2006). NOAA Atlas 14: Precipitation-Frequency Atlas of the United States. http://hdsc.nws.noaa.gov/hdsc/pfds/pfds_printpage.html?lat=36.8472&lon=-75.9833&data=intensity&units=metric&series=pds. Accessed Aug 2016.

Ciach, G. J. and Krajewski, W. F. (2006). Analysis and modeling of spatial correlation structure in small-scale rainfall in Central Oklahoma. *Advances in Water Resources*, 29(10):1450–1463.

Emmanuel, I., Andrieu, H., Leblois, E., and Flahaut, B. (2012). Temporal and spatial variability of rainfall at the urban hydrological scale. *Journal of Hydrology*, 430-431:162–172.

Ercan, M. B. and Goodall, J. L. (2013). Estimating Watershed-Scale Precipitation by Combining Gauge- and Radar-Derived Observations. *Journal of Hydrologic Engineering*, 18(8):983–994.

Ezer, T. and Atkinson, L. P. (2014). Accelerated flooding along the U.S. East Coast: On the impact of sea-level rise, tides, storms, the Gulf Stream, and the North Atlantic Oscillations. *Earth's Future*, 2(8):362–382.

Fletcher, T., Andrieu, H., and Hamel, P. (2013). Understanding, management and modelling of urban hydrology and its consequences for receiving waters: A state of the art. *Advances in Water Resources*, 51:261–279.

Galarneau, T. J., Davis, C. A., and Shapiro, M. A. (2013). Intensification of Hurricane Sandy (2012) through Extratropical Warm Core Seclusion. *Monthly Weather Review*, 141(12):4296–4321.

Goovaerts, P. (2000). Geostatistical approaches for incorporating elevation into the spatial interpolation of rainfall. *Journal of Hydrology*, 228(1-2):113–129.

Hall, M. (1984). *Urban hydrology.* Elsevier Applied Science, Barking, UK.

Hayward, D. and Clarke, R. T. (1996). Relationship between rainfall, altitude and distance from the sea in the Freetown Peninsula, Sierra Leone. *Hydrological Sciences Journal*, 41(3):377–384.

Hill, D., Kerkez, B., Rasekh, A., Ostfeld, A., Minsker, B., and Banks, M. K. (2014). Sensing and Cyberinfrastructure for Smarter Water Management: The Promise and Challenge of Ubiquity. *Journal of Water Resources Planning and Management*, 140(7):01814002.

Hill, D. J. (2015). Assimilation of weather radar and binary ubiquitous sensor measurements for quantitative precipitation estimation. *Journal of Hydroinformatics*, 17(4):598.

Homer, C. G., Dewitz, J. A., Yang, L., Jin, S., Danielson, P., Xian, G., Coulston, J., Herold, N. D., Wickham, J., and Megown, K. (2015). Completion of the 2011 National Land Cover Database for the conterminous United States-Representing a decade of land cover change information. *Photogramm. Eng. Remote Sens*, 81(5):345—-354.

Jensen, N. and Pedersen, L. (2005). Spatial variability of rainfall: Variations within a single radar pixel. *Atmospheric Research*, 77(1):269–277.

Kates, R. W., Colten, C. E., Laska, S., and Leatherman, S. P. (2006). Reconstruction of New Orleans after Hurricane Katrina: a research perspective. *Proceedings of the National Academy of Sciences of the United States of America*, 103(40):14653–60.

Kebaili Bargaoui, Z. and Chebbi, A. (2009). Comparison of two kriging interpolation methods applied to spatiotemporal rainfall. *Journal of Hydrology*, 365(1):56–73.

Krajewski, W. and Smith, J. (2002). Radar hydrology: rainfall estimation. *Advances in Water Resources*, 25(8):1387–1394.

Krajewski, W. F., Ciach, G. J., and Habib, E. (2003). An analysis of small-scale rainfall variability in different climatic regimes. *Hydrological Sciences Journal*, 48(2):151–162.

Nesbitt, S. W. and Anders, A. M. (2009). Very high resolution precipitation climatologies from the Tropical Rainfall Measuring Mission precipitation radar. *Geophysical Research Letters*, 36(15).

Nicholls, R. J. and Cazenave, A. (2010). Sea-level rise and its impact on coastal zones. *Science (New York, N.Y.)*, 328(5985):1517–20.

NOAA (2017). NEXRAD Products. https://www.ncdc.noaa.gov/data-access/radar-data/nexrad-products. Accessed Jan 2017.

O'Gorman, P. A. and Schneider, T. (2009). The physical basis for increases in precipitation extremes in simulations of 21st-century climate change. *Proceedings of the National Academy of Sciences*, 106(35):14773–14777.

Overeem, A., Leijnse, H., and Uijlenhoet, R. (2013). Country-wide rainfall maps from cellular communication networks. *Proceedings of the National Academy of Sciences of the United States of America*, 110(8):2741–5.

Pedersen, L., Jensen, N. E., Christensen, L. E., and Madsen, H. (2010). Quantification of the spatial variability of rainfall based on a dense network of rain gauges. *Atmospheric Research*, 95(4):441–454.

Renard, D., Bex, N., Desassis, N., Beucher, H., Ors, F., and Laporte, F. (2015). RGeostats: The Geostatistical package. Free download from: http://cg.ensmp.fr/rgeostats. Accessed Jul 2016.

Rotzoll, K. and Fletcher, C. H. (2012). Assessment of groundwater inundation as a consequence of sea-level rise. *Nature Climate Change*, 3(5):477–481.

Seo, D.-J. (1998). Real-time estimation of rainfall fields using radar rainfall and rain gage data. *Journal of Hydrology*, 208(1-2):37–52.

Serinaldi, F. (2008). Analysis of inter-gauge dependence by Kendall's τK, upper tail dependence coefficient, and 2-copulas with application to rainfall fields. *Stochastic Environmental Research and Risk Assessment*, 22(6):671–688.

Smith, J. A., Baeck, M. L., Meierdiercks, K. L., Miller, A. J., and Krajewski, W. F. (2007). Radar rainfall estimation for flash flood forecasting in small urban watersheds. *Advances in Water Resources*, 30(10):2087–2097.

Smith, J. A. and Krajewski, W. F. (1993). A modeling study of rainfall rate-reflectivity relationships. *Water Resources Research*, 29(8):2505–2514.

Suarez, P., Anderson, W., Mahal, V., and Lakshmanan, T. (2005). Impacts of flooding and climate change on urban transportation: A systemwide performance assessment of the Boston Metro Area. *Transportation Research Part D: Transport and Environment*, 10(3):231–244.

Sun, X., Mein, R., Keenan, T., and Elliott, J. (2000). Flood estimation using radar and raingauge data. *Journal of Hydrology*, 239(1-4):4–18.

Sweet, W., Park, J., Marra, J., Zervas, C., and Gill, S. (2014). Sea Level Rise and Nuisance Flood Frequency Changes around the United States. *NOAA Technical Report NOS CO-OPS 073*, (June):58.

Titus, J. G., Kuo, C. Y., Gibbs, M. J., LaRoche, T. B., Webb, M. K., and Waddell, J. O. (1987). Greenhouse Effect, Sea Level Rise, and Coastal Drainage Systems. *Journal of Water Resources Planning and Management*, 113(2):216–227.

U.S. Department of Commerce (2012). Virginia: 2010, Population and Housing Unit Counts. https://www.census.gov/prod/cen2010/cph-2-48.pdf. Accessed Aug 2016.

Velasco-Forero, C. A., Sempere-Torres, D., Cassiraga, E. F., and Jaime Gómez-Hernández, J. (2009). A non-parametric automatic blending methodology to estimate rainfall fields from rain gauge and radar data. *Advances in Water Resources*, 32(7):986–1002.

Wu, W., Kitzmiller, D., Wu, S., Wu, W., Kitzmiller, D., and Wu, S. (2012). Evaluation of Radar Precipitation Estimates from the National Mosaic and Multisensor Quantitative Precipitation Estimation System and the WSR-88D Precipitation Processing System over the Conterminous United States. *Journal of Hydrometeorology*, 13(3):1080–1093.

Zinevich, A., Alpert, P., and Messer, H. (2008). Estimation of rainfall fields using commercial microwave communication networks of variable density. *Advances in Water Resources*, 31(11):1470–1480.